Physical interpretation of impacts from a low cost manufacturing process on the surface microstructure of a novel solar absorber

P. Konttinen[*], P. D. Lund

Advanced Energy Systems Laboratory, Helsinki University of Technology, P.O.Box 2200, FIN-02015 HUT, Finland

Abstract

A novel lower cost mechanical solar absorber manufacturing method has been developed. $C/Al_2O_3/Al$ surfaces have been characterized with optical and microstructural methods. The surface consists of thin inhomogeneous matrix containing carbon and Al_2O_3 on Al-substrate. Manufacturing of the surface can be done by single phase manual or mechanical grinding with a silicon carbide grinding pad. A solar absorptance $\alpha = 0.90$ and a thermal emittance $\varepsilon = 0.22$ have been achieved so far. Durability and aging mechanisms of the surface have been determined in laboratory and test field. The $C/Al_2O_3/Al$ surface has passed accelerated aging tests recommended by IEA-SHC for high temperature and combined elevated temperature and condensation. The main degradation mechanism is hydration of aluminium oxide. The estimated service lifetime of the absorber (with an optical performance more than 95% of its initial) in normal use is in the range of $20 - 25$ years, depending on the condensation frequency distribution on the surface. Computer simulations and solar collector testing at test field demonstrate some 5-17% lower annual energy yield compared to the commonly used collectors with nickel-pigmented and sputtered absorbers.

Keywords: low cost solar absorber, mechanical manufacturing, $C/Al_2O_3/Al$

1. Introduction

The best available commercial technologies, e.g. sputtering enable production of absorber surfaces with almost optimal optical properties [1-3]. However, sputtered absorbers can be quite expensive. Selective paints [4-5] and nickel nano-particle containing paint [6] may provide a promising low-cost manufacturing method. Another environmentally friendly low-cost method can be mechanical manufacturing. The purpose of this study is to update and combine the relevant aspects of the mechanical method containing manufacturing, microstructural and optical analysing, durability and performance of the selective $C/Al_2O_3/Al$ surface. The surface consists of heterogeneous matrix containing carbon (possibly in graphite form) and Al_2O_3 on Al-substrate [7]. The manufacturing process has been developed from manually operated abrasive grinding followed with an acid bath to a mechanically operated grinding alone [8].

Previous theoretical and practical studies of manufacturing a solar absorber by combining a graphite layer with rough surface have been published by Botten and Ritchie [9] and Golomb [10], respectively. An early work about using mechanical grinding to increase the selectivity of surfaces prior to deposition of multilayer interference coating has been reported by Kudryashova [11]. The manufacturing method described in this paper differs from these in that it utilizes mechanical grinding for forming the selective surface without further treatments. The main concept is to roughen the Al surface and add an absorptive layer on it simultaneously.

---

[*] Corresponding author: Tel: +358 9 451 3212; Fax: +358 9 451 3195; e-mail: petri.konttinen@hut.fi

2. Manufacturing methods

Selective $C/Al_2O_3/Al$ surfaces can be manufactured with several different processes [7-8]. In the beginning, manual grinding was preferred over mechanical grinding because even small changes in the manufacturing parameters (speed, time, pressure, grinding pattern) gave completely different results for optical parameters and surface homogeneity. Optical properties of the surfaces were characterized for identifying the grinding practices which provided with the highest α and lowest ε [7-8]. The best practice manual manufacturing parameters were determined in order to convert the process into mechanically operated grinding.

The mechanical grinding is typically done on 99.5% pure Al-substrate sheets with dimensions: 2 x 0.12 x 0.005 m. The latest version of the method implements an electrical control and a guiding mechanism: A non-correlating classical random noise signal generates the control voltage for the X/Y –electromagnetic control units of the grinding unit (Fig. 1a). The grinding unit drives a grinding pad attached to a wheel head (Fig. 1b). As a result, the grinding pad moves locally across the Al-substrate 2-dimensionally with variable speed (from zero to 20 m s^{-1}) and direction forming a 2-dimensional grinding pattern on the surface. In order to obtain a homogeneous pattern over the whole surface, the Al-substrate sheet moves back and forth under the grinding unit in a relatively slow motion (less than 1 m s^{-1}). A typical process lasts for about 15 minutes.

Very hard grinding particles, e.g. silicon carbide are attached in the grinding pad thus forming a 3-dimensional matrix. The size of the particles varies and is typically between ~300 nm - 2 µm. While the pad wears, new particles come into touch with the surface of the absorber substrate, increasing the uniformity of the process. During the manufacturing process the grinding pad is saturated with carbon dust, which is bound to the pad by static electricity. Carbon dust reacts with the surface being scratched and atmospheric oxygen forming a heterogeneous carbon and alumina matrix structure on the final surface.
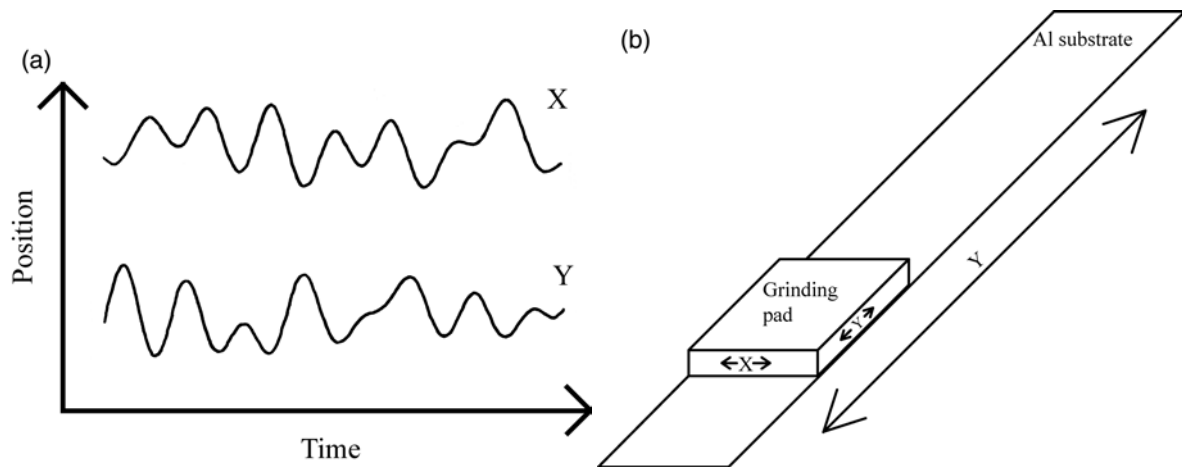

Figure 1. The non-correlating classical random noise moves the grinding pad in X/Y -directions across the Al substrate sheet (a and b). The substrate moves back and forth slowly in Y-dimension (b, not on scale).

3. Surface characterization

3.1 Optical characterization

The solar absorptance α of the $C/Al_2O_3/Al$ samples have been determined from 0.39 to 1.1 μm with a LI-COR LI-1800 type spectroradiometer and an integrating sphere [7-8, 12-13]. The infrared emittance ε have been determined from 2.5 to 20 μm with a MIDAC Prospect IR type FTIR-spectrometer. Reference measurements for some of the samples have been done at the Ångström laboratory of the Uppsala University (Fig. 2). The best combination of optical properties obtained so far with mechanical manufacturing are: $\alpha = 0.90$ and $\varepsilon = 0.22$ [7]. No higher α than 0.91 have been measured.
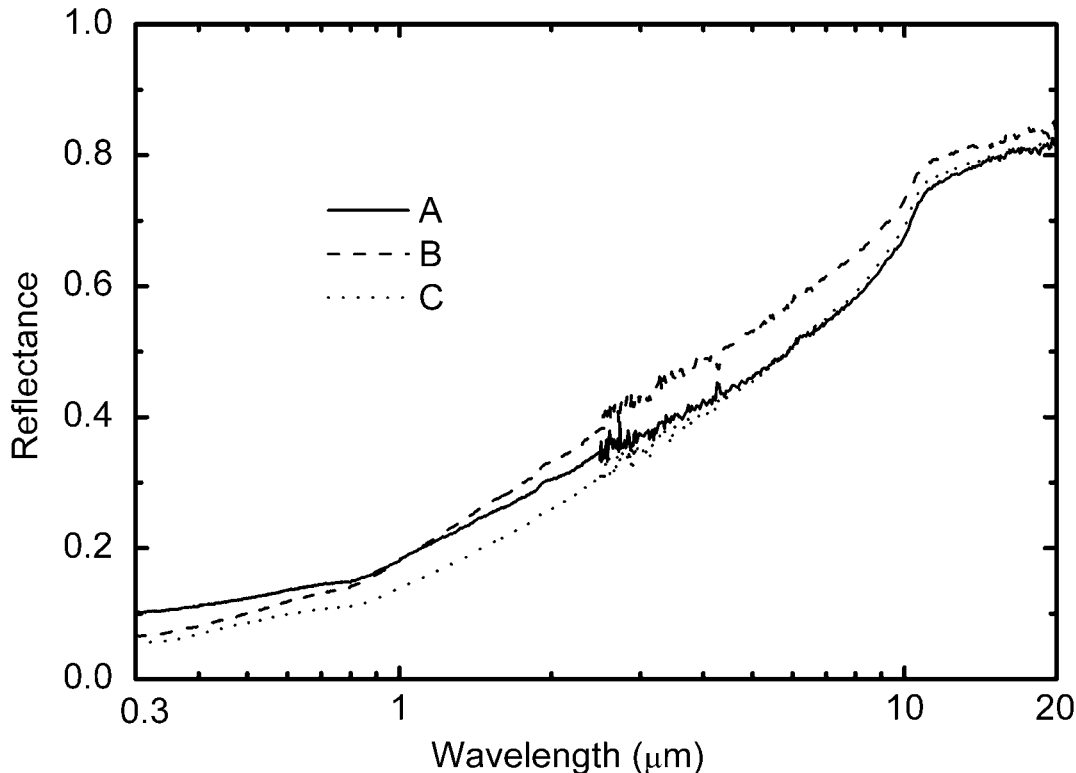

Figure 2. Spectral reflectance of three $C/Al_2O_3/Al$ surface samples A, B and C. The corresponding optical properties are: $0.83 \leq \alpha \leq 0.87$ and $0.25 \leq \varepsilon \leq 0.29$ [8].

3.2 Microstructural characterization

The microstructure of the surface contains inhomogeneous grooves with a typical width of 1-2 μm. An example of how the microgrooves are organized on a typical sample surface is shown in Fig. 3a. Optical microscopy revealed that the surface is inhomogeneously covered by a dark layer [7], which have been confirmed by EDS as carbon. Based on XPS analyses it is possible that the carbon is mainly in graphite form [7].

In Fig. 3a on an area of about 50 x 40 μm are visible a few approximately 2 μm wide grooves, which are clearer and sharper on the edges compared to the narrower grooves. This can be explained by the size of the silicon carbide particles (300 nm - 2 μm) of the grinding pad and the nature of the grinding process. Particle size below 1 - 1.5 μm most probably constitutes a majority of the particle frequency distribution thus resulting in the majority of the groove widths being in the

range of 1 μm. As the surface is being grinded over multiple times during the whole manufacturing period (e.g. 15 min), only the latest formed grooves remain sharp-edged.

Fig. 3b shows an optical microscopy photograph of a surface (denoted as surface 25 in [7]) having $\alpha = 0.90$ and $\varepsilon = 0.22$. It must be noted that the optical resolution of the optical microscope and resolution of the CCD-camera used for obtaining Fig. 3b prohibits analyses of objects of size smaller than approximately 1-2 times the wavelength of incident light. For example, the observed contrast between topographic microgrooves and plateaus of the same magnitude might occur only because of light trapping in the grooves themselves irrespectively of any absorbing carbon layer.
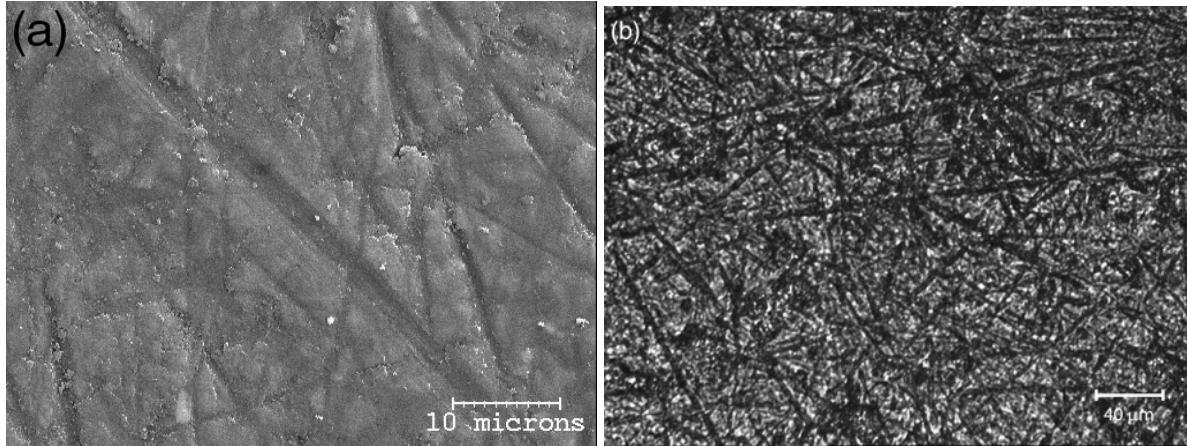

Figure 3: SEM micrograph (a) and optical microscope photograph (b) of two typical surface samples. Surface (b) is denoted as surface 25 in [7]. AFM micrograph of different area of the same surface sample is shown in Fig. 5.

Fig. 4 shows a crosscut field emission scanning electron microscopy (SEM) micrograph of a typical surface sample [7]. The sample was manufactured by placing a crosscut section of a surface sample between two pieces of stainless steel (SS) and casting it in epoxy, which was sawed in half and the crosscut section was manually diamond-polished. Areas denoted as 3 most likely show an interface layer between the Al substrate and SS-layer.

Atomic force microscopy (AFM) was used in order to determine the 3-dimensional structure of the surface in Fig. 3b in more detail. The equipment consists of a Danish Micro Engineering DME Rasterscope 4000™. The maximum measuring area is 50 x 50 μm. Fig. 5 shows typical 2- and 3-dimensional AFM micrographs of the surface and three cross section profiles (denoted as 1-3). The width of the three microgrooves visible within profiles 1-3 is approximately 0.7-1.2 μm. Microgroove profiles are clearly distinguishable from cross section profiles 1-2: At the approximate height of 200 nm (80 nm from the groove bottom) both profiles becomes sharply broader on one side indicating the end of a clearly separate single microgroove. In contrast profile 3 has a knifelike sharp V-form having a height of 160 nm from the groove bottom. These results indicate that the surface has microgrooves with variable sharpness and a depth of approximately 80-160 nm. The total difference in elevation is approximately 400 nm, which is typical for this surface (based on all the other AFM analyses as well).
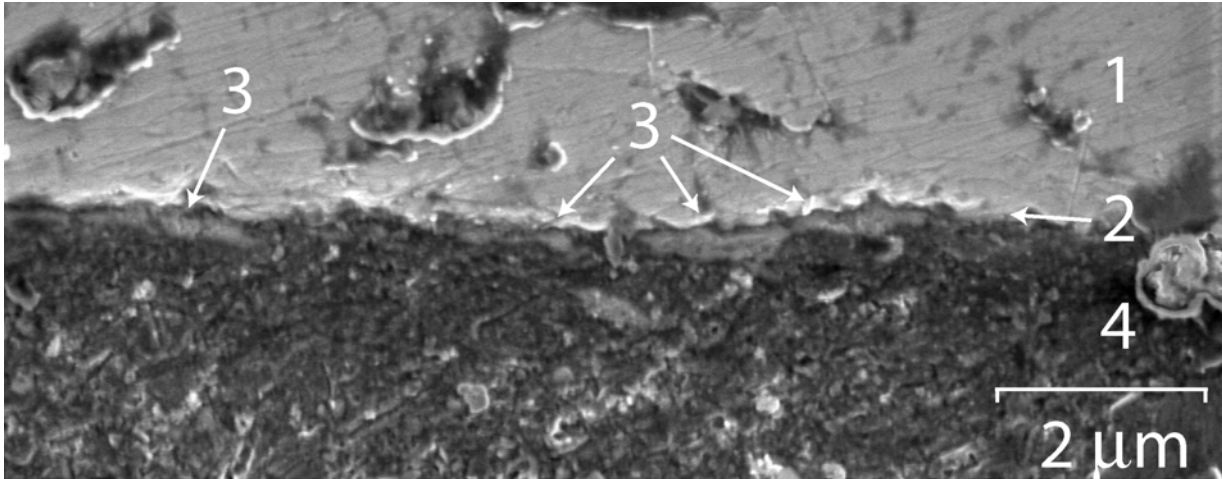
Figure 4. A crosscut field emission SEM micrograph of a typical surface sample. 1) stainless steel (SS) attached on top of the surface before crosscutting, 2) surface borderline between the SS and Al$_2$O$_3$ layers, 3) areas that can be interpreted as an interface layer between the Al-substrate and SS-layer, 4) Al substrate.

3.3 Comparison to literature

Botten and Ritchie [9] have theoretically studied improving of a solar absorber surface by surface roughening, which enables the use of a grating absorption phenomenon known as surface plasmons. They used an idealized graphite layer with a refractive index of $1.95 + 0.34i$ and a sinusoidal profile single dimensional uniform graphite-copper interface grating. The best α achieved was 86% (unspecified air mass) with $\varepsilon = 41\%$ (at 700K) for uniform graphite film thickness of 0.4 µm. With 0.3 µm thick graphite layer α was 84% and ε was 25%. Values of $0.81 \leq \alpha \leq 0.91$ (AM 1.5) and $0.22 \leq \varepsilon \leq 0.46$ (373K) have been measured for the mechanically manufactured C/Al$_2$O$_3$/Al samples [7-8]. Raising the emitter temperature from 373K to 700K raises the calculated ε of the C/Al$_2$O$_3$/Al samples some 0.15, which still in some cases fits within the results for 0.4 µm thick uniform graphite film thickness by Botten and Ritchie. The estimated carbon/graphite film of C/Al$_2$O$_3$/Al samples is not uniformly thick and covering, nor does it form a sinusoidal profile. However, Botten and Ritchie predicted that an arbitrary form of roughening would produce results similar to those for sinusoidal form. Botten and Ritchie calculated that with an optimized diffraction gratings optical properties of $\alpha = 0.884$ and $\varepsilon = 0.062$ would be obtainable. The parameters are: a mean graphite thickness of 0.12 µm, the depth of roughening of 0.15 µm and a roughness period of 0.5 µm.

Golomb [10] have experimentally studied interference films, silicon on aluminium and graphite on copper, which were deposited by electron beam evaporation on holographically produced diffraction gratings and meshes. Most of his study concentrates on silicon on aluminium systems. He noticed a strong plasmon effect in his experiments, for graphite copper system raising α from 0.79 to 0.88 while leaving ε constant at 0.04. The parameters used were: roughness period 0.642 µm, graphite thickness 0.12 µm and groove depth 0.17 µm. Compared to a plane interface with the same graphite thickness the solar reflectance was approximately halved while ε was increased by < 0.01. Golomb experienced that biperiodic surfaces have slightly greater α than uniperiodic surfaces. This feature implied that a randomly roughened surface might be even more absorbing than the corresponding uniperiodic surface, which is in accordance with the results by Botten and Ritchie [9].
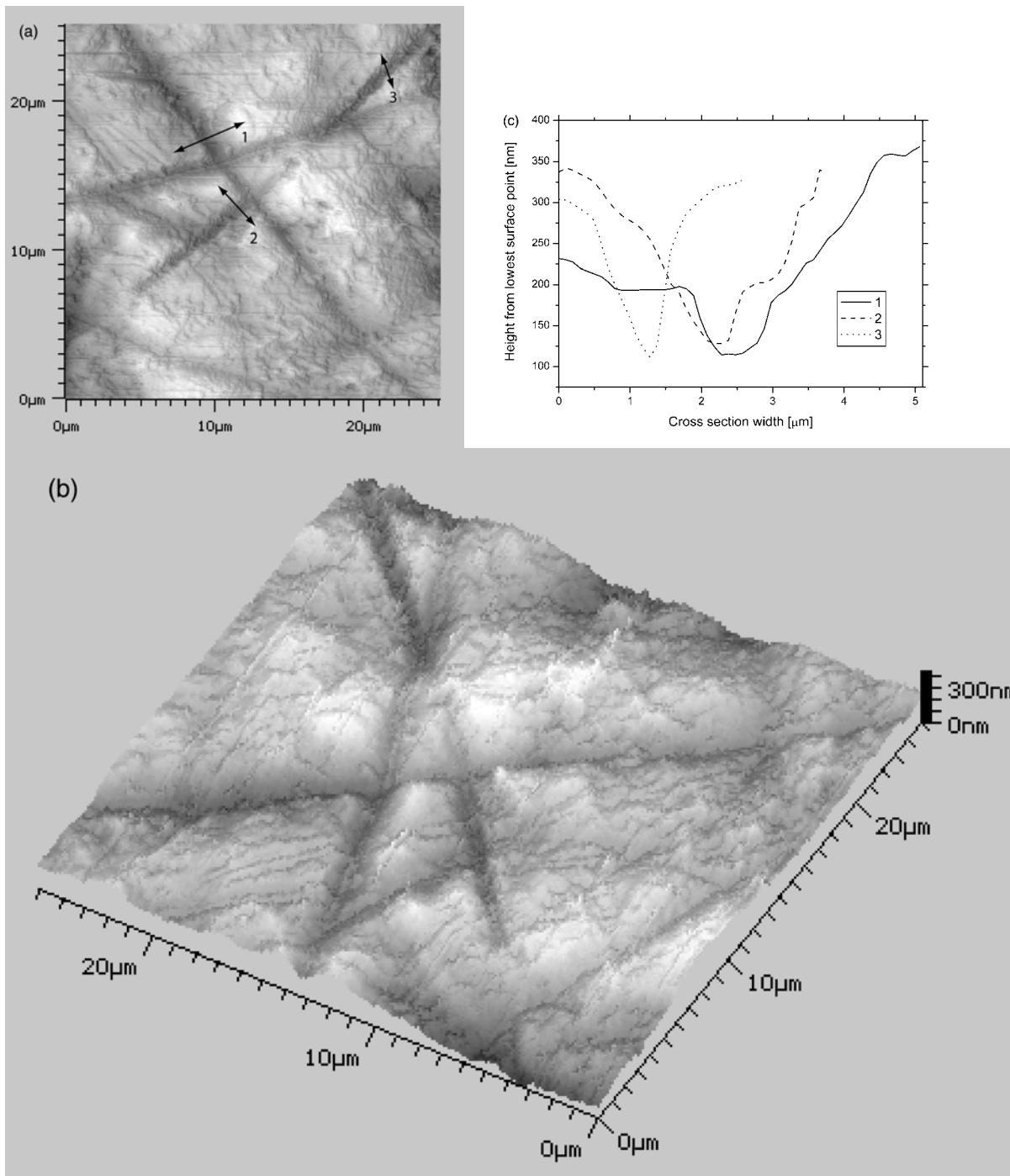
Figure 5. 2D (a) and 3D (b) AFM micrographs of an absorber sample having $\alpha = 0.90$ and $\varepsilon = 0.22$ (denoted as surface 25 in [7]). Cross section profiles of three microgrooves (c). Surface area is 25 x 25 μm. Optical photograph of different area of the same surface sample is shown in Fig. 3b.

6

4. Accelerated aging tests

Samples of $C/Al_2O_3/Al$ absorber surfaces were subjected to accelerated aging tests in order to determine their expected service lifetime (with an optical performance more than 95% of its initial). High temperature and combined elevated temperature/condensation tests were mainly performed according to the IEA SHC recommendations (draft ISO/DIS 12592) [14-16] with some additional tests. Full results will be published in Sol. Energy Mater. Sol. Cells [13]. Standard SO_2 –tests were not performed due to absence of the equipment needed, but they have been replaced with more severe tests: Absorber samples are subjected to simulated acid rain containing sulphuric acid at temperature range of 60-100°C and duration up to 14 days. The results will be published separately after concluding the tests.

Carlsson et al. [17-18] reported that one main degradation mechanism of nickel-pigmented anodized aluminium absorber coating is hydration of aluminium oxide to pseudoboehmite ($AlO \cdot OH \cdot XH_2O$, X=0.4–1) and to boehmite (γ–$AlO \cdot OH$). Results from aging tests indicate that a hydration mechanism similar to the one degrading nickel-pigmented anodized aluminium absorber coating is affecting the mechanically manufactured $C/Al_2O_3/Al$ absorber surfaces as well [13].

We calculated service lifetime estimates for the $C/Al_2O_3/Al$ absorber surface based on the assumption that the hydration process is the only significant active degradation process during the service lifetime of the collector. High temperature (200h at 250°C) alone does not degrade the surfaces. In addition, the surfaces have been found to be insensitive to extensive UV irradiation as well, and to withstand 383 days of temperature and irradiance cycling with total irradiance level of 1000-7000 W m^{-2} and temperature range of -40°C…120°C [19]. The average service lifetime estimate based on activation energies from two literature sources [17, 16] is 20 and 25 years, respectively [13]. The main cause in the variation in service lifetime estimates is the divergence of the time of wetness frequency distribution between the literature sources.

5. Discussion

Efforts should be made in order to optimize the composition of the grinding pad and adjusting the grinding parameters accordingly to produce surfaces having surface layer thickness and periodicity close to those obtained by Botten and Ritchie [9] and Golomb [10]. Further improvements in the absorber structure could include use of antireflection (AR) coating. A possible low-cost antireflection coating option could be colloidal silica dipping AR-coating [20-22]. If an AR-coating could be enhanced to act as a moisture barrier layer as well, it would add moisture resistance for very humid climates. However, the antireflection/moisture barrier -coating needs to be inexpensive in order to keep the original $C/Al_2O_3/Al$ absorber manufacturing concept low-cost.

The manufacturing cycle delivery time could be shortened from 15 minutes if more suitable grinding pads would be available. However, this has not been considered a major issue so far, as parallel grinding units can be used for manufacturing several sheets at the same time, and their number can be scaled up inexpensively (a few kiloeuros per unit).

It might be possible that the interface layer shown in Fig. 3 contains separate carbon or graphite clusters (see [7] for more details), but there could be intermixed carbon-alumina layers as well, or even other carbon compounds. Several field emission SEM and EDS analyses have been conducted for three different cross-section samples. It has not been possible to positively identify the elemental composition of this kind of interfaces with any of these analyses. The absorber surface contains thicker than natural alumina layer [7], which could be separately under the carbon layer or intermixed with the carbon during the mechanical grinding. One possibility is that the mechanical manufacturing process first adds a relatively thick alumina layer on the Al-substrate, and only after this carbon layer is formed. This theory is supported to some extent visual observation of typical absorber manufacturing, where the colour of the substrate does not change significantly during the

first ~10 minutes of the whole 15 minutes period. Another possibility is that the surface contains an intermixture of carbon and Al_2O_3. In any case, no reliable estimation of the thickness of the Al_2O_3 layer can be made based on the analyses conducted so far.

It is likely that during the hydration process the carbon layer on the surface is oxidised through chemical reactions forming CO, CO_2 and other compounds [23]. The revealed Al_2O_3 layer subsequently follows the typical alumina-aluminium corrosion mechanisms.

The energy production of a solar collector containing $C/Al_2O_3/Al$ absorbers has been estimated by dynamic collector testing [19] and computer simulations. The results indicate some 5-17% lower energy yield compared to the commercially available solar collectors with the same dimensions. The 5% difference was dynamically measured against a nickel-pigmented selective anodized aluminium absorber collector in Espoo, Finland (Fig. 6). The 17% lower annual energy yield and 11% lower annual solar fraction against a commercial collector containing sputtered surface on a copper substrate was calculated for a typical Central European climate by a computer simulation [8]. The values of the optical parameters for the $C/Al_2O_3/Al$ absorber were: $\alpha = 0.90$, $\varepsilon = 0.25$.
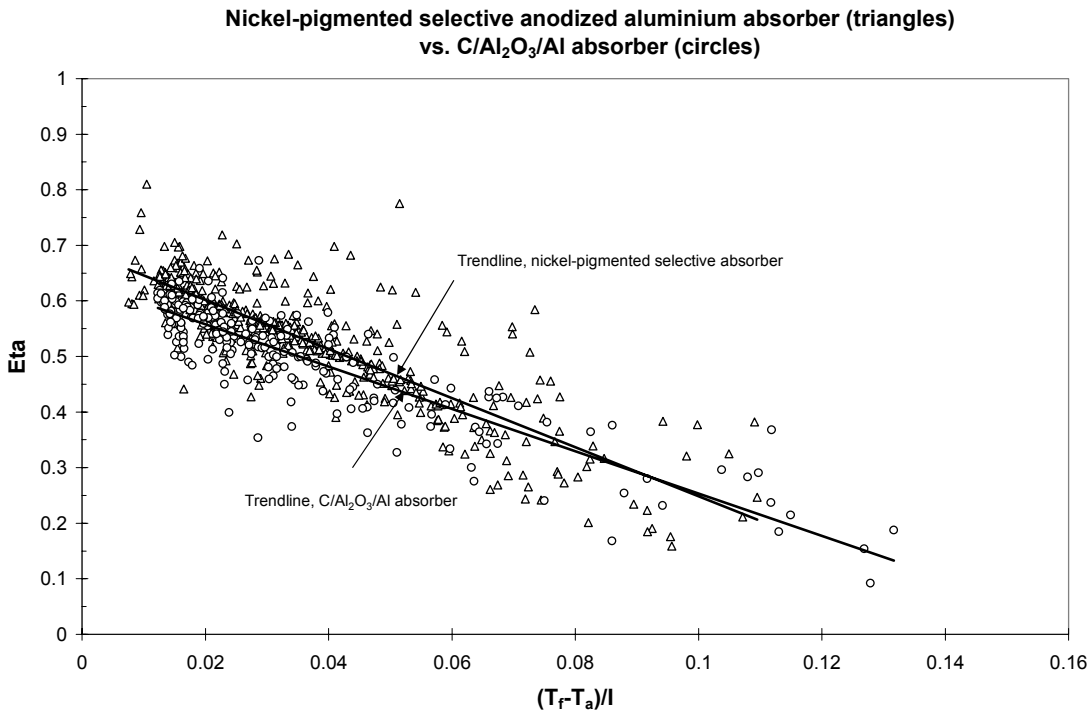

Figure 6. Dynamically measured solar collector efficiency points as a function of $(T_f-T_a)/I$. Data for a $C/Al_2O_3/Al$ absorber and a selective nickel-pigmented anodized aluminium absorber shown. T_f is the average collector fluid temperature, T_a is the ambient temperature and I is the total irradiance onto the collector plane. Collector area 2.3 m^2, measured at the Helsinki University of Technology solar energy test site in Otaniemi, Espoo, Finland (60°11'N, 24°50'E).

6. Conclusions

The selective $C/Al_2O_3/Al$ absorber surface at the present stage of development is suitable for middle quality and lower cost solar heating system, operating at low to medium temperatures. The price of the manufacturing equipment needed is very low and the number of absorber sheets

manufactured simultaneously can be scaled up inexpensively. α of 0.90 and ε of 0.22 have been achieved so far.

The $C/Al_2O_3/Al$ surface has passed accelerated aging tests recommended by IEA-SHCP [14] for high temperature and combined elevated temperature and condensation [13]. Based on the reference data from two sources we estimated the service lifetime of the collector to be 20 – 25 years in normal use before the performance have degraded by 5%. The estimated service lifetime depends significantly on the condensation frequency distribution on the surface. The main degradation form is hydration of aluminium oxide due to presence of condensed water on the surface. Failures in collector cover or pipe layout leading to increased humidity on the absorber surface present severe risk to the absorber lifetime.

The energy production of a solar collector with $C/Al_2O_3/Al$ absorbers at the present stage of development is estimated to be some 5-17% lower compared to the commercially available solar collectors with the same dimensions.

References

[1] T. Eisenhammer, A. Mahr, A. Haugeneder, and W. Assmann, Sol. Energy Mater. Sol. Cells 46 (1997) 53-65.
[2] E. Wäckelgård and G. Hultmark, Sol. Energy Mater. Sol. Cells. 54 (1998) 165-170.
[3] M. Farooq, and M.G. Hutchins, Sol. Energy Mater. Sol. Cells 71 (2002) 523-535.
[4] Z.C. Orel and M.K. Gunde, Sol. Energy Mater. Sol. Cells 68 (2001) 337-353.
[5] G.B. Smith, A. Gentle, P.D. Swift, A. Earp and N. Mronga, Sol. Energy Mater. Sol. Cells. 79 (2003) 163-177
[6] T. Boström, E. Wäckelgård and G. Westin, Solar Energy 74 (2003) 497-503.
[7] P. Konttinen, R. Kilpi and P.D. Lund, Thin Solid Films 425 (2003) 24-30.
[8] P. Konttinen, P.D. Lund, and R.J. Kilpi, Sol. Energy Mater. Sol. Cells 79 (2003) 273-283.
[9] L.C. Botten and I.T. Ritchie, Opt. Commun. 23 (1977) 421-426.
[10] M. Golomb, Opt. Commun. 27 (1978) 177-180.
[11] M.D. Kudryashova, Appl. Solar Energy 5 (1969) 24-25.
[12] P. Konttinen and P.D. Lund, World Renewable Energy Congress VII, 29 June - 5 July 2002, Cologne, Germany.
[13] P. Konttinen and P.D. Lund, Thermal stability and moisture resistance of $C/Al_2O_3/Al$ solar absorber surfaces. Sol. Energy Mater. Sol. Cells, accepted for publication
[14] S. Brunold, U. Frei, B. Carlsson, K. Möller and M. Köhl, Sol. Energy 68 (2000) 313-323.
[15] B. Carlsson, K. Moller, M. Kohl, U. Frei and S. Brunold, Sol. Energy Mater. Sol. Cells 61 (2000) 255-275.
[16] M. Köhl, Renewable Energy 24 (2001) 597 – 607.
[17] B. Carlsson, U. Frei, M. Köhl and K. Möller, Accelerated Life Testing of Solar Energy Materials - Case study of some selective materials for DHW-systems, IEA SHCP Task X, 1994
[18] B. Carlsson, K. Moller, U. Frei, S. Brunold and M. Kohl, Sol. Energy Mater. Sol. Cells 61 (2000) 223-238.

[19] P. Konttinen, Lic.Sc. Thesis, Department of Engineering Physics and Mathematics, Helsinki University of Technology, Finland, 2000.

[20] T. Tesfamichael and A. Roos, Sol. Energy Mater. Sol. Cells 54 (1998) 213-221.

[21] P. Nostell, A. Roos and B. Karlsson, Thin Solid Films 351 (1999) 170-175.

[22] A. Gombert, W. Glaubitt, K. Rose, J. Dreibholz, B. Blasi, A. Heinzel, D. Sporn, W. Doll and V. Wittwer, Solar Energy 68 (2000) 357-360.

[23] L.H. Hihara and R.M. Latanision, Int. Mater. Rev. 39 (1994) 245-264.